DYNAMICS OF FAST AXONAL TRANSPORT

IRVING NADELHAFT

From the Veterans Administration Hospital, Pittsburgh, Pennsylvania 15240, and the Department of Neurological Surgery, University of Pittsburgh Medical School, Pittsburgh, Pennsylvania 15261

ABSTRACT A phenomenological model of the process of fast axoplasmic transport is presented. The process was conceived of as occurring in two parts: (*a*) synthesis and storage of material in a cytoplasmic pool; (*b*) release from the pool and transport distally along the axon. Considering the fate of labeled proteins, the activity at points along the axon reflects events occurring earlier within the pool through the relationship: $g(x,t) = \text{const} f(t - x/v)$; where $g(x,t)$ represents axonal activity, $f(t)$ the pool's activity, and v is the transport speed. Using the idea that when there is no further input of radioactivity into the pool its activity declines exponentially due to export of material to the axon, I generalized this concept to the case where activity enters and leaves the pool simultaneously. The model contains two parameters: the relative turnover rate of the pool, α, and T, an interval characteristic of the time of synthesis. From this model, the experimental data is unfolded and yields values for these parameters of $\alpha = 0.004\ \text{min}^{-1}$ and $T \approx 60$ min.

The phenomenon of fast axonal transport has been extensively examined in the sciatic nerve of mammals (usually cats) by Ochs and his co-workers (Ochs et al., 1970; Ochs, 1972*a*). As shown in Fig. 1, the profile of activity along the nerve distal to the injected dorsal root ganglion (L7) has several characteristic features: a peak (A) which coincides with the position of the ganglion, a distal crest (B), and two sloping regions (C and D). Based upon a model for the synthesis-flow process, I attempted an explanation for the shape of this downflow profile, and, in addition, extracted numerical values estimating the parameters of the model from the data. A qualitative picture describing these events has already been proposed by Ochs (1972*b*). The two models overlap each other and are complementary rather than alternative explanations of the phenomena they describe.

The following assumptions were made: (*a*) synthesis is confined to the cell soma, (*b*) no losses occur as material moves distally (corrections for this can easily be made), (*c*) only fast flow will be considered, (*d*) although the sciatic nerve contains many fibers, the model lumps them all together treating the nerve as one fiber and one cell body; this simplification amounts to treating the average fiber. Fig. 2 provides a pictorial framework for the model. The proteins that are exported come from a pool, which contains a number, assumed to be constant at N, of protein molecules. These are continually replenished at a rate $\dot{N}$ as they leave to move axodistally. The turnover of the pool can be described by a single number $\alpha = \dot{N}/N$ = "relative turnover rate." When some of the pool proteins are labeled, this information is contained in a function $f(t)$

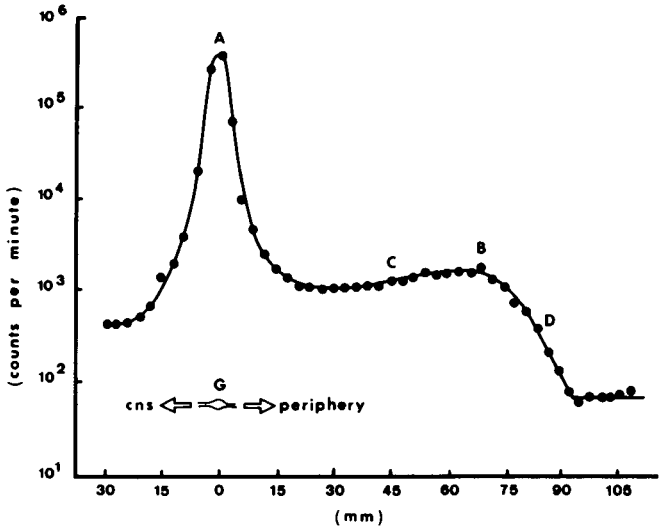

FIGURE 1 Example of a typical downflow profile. [^{3}H]leucine was injected into the L7 dorsal root ganglion (G). The sciatic nerve was removed after 5 h, divided into 3-mm pieces, and counted in a liquid scintillation counter. The letters A–D are explained in the text. This figure was adapted from Fig. 5 of Ochs et al. (1970) with the permission of the authors and publisher.

representing the fraction which are labeled: $f(t) = N^*/N$, where N^* is the number of labeled molecules. $f(t)$ changes for two reasons: (*a*) those proteins leaving carry away some label, thus reducing f, and (*b*) incoming proteins bring in some label, thus increasing f. If after a certain time, no more labeled proteins enter the pool, the pool activity will decline as time passed due to the continual exit of label. If f_o is the value of the pool fraction at that time, then this decline is given by

$$f(t) = f_o e^{-\alpha t}. \tag{1}$$

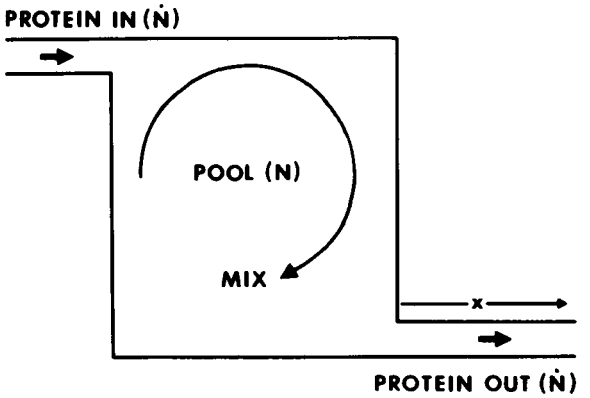

FIGURE 2 Schematic representation of the model. Proteins manufactured within the somal cytoplasm are transferred to the cytoplasmic pool (N molecules) at a rate $\dot{N}$ and are exported axodistally along the axon from the origin at the cell soma.

As will be shown below, this simple time dependence can be used to generate the more complex behavior of $f(t)$ expected when labeled proteins are simultaneously entering and leaving the pool.

I turn first, however, to a consideration of the relationship between the downflow profile, as exhibited in the axon, and the pool fraction f. During an interval of time Δt, the number of labeled molecules leaving the pool is $\Delta N^* = f(t)\,\Delta N = f(t)\dot{N}\Delta t$. This number occupies a linear distance along the axon given by $\Delta x = v\Delta t$, where v is the speed of transport. Consider the profile of counts in the axon at an arbitrary time t, after the ganglion has been injected. Let this profile be described by the function $g(x,t)$ so that the number of counts at the position $(x, \Delta x)$ is given by $G(x,t) = g(x,t)\,\Delta x$. This activity was exported from the pool at an earlier time $t' = t - x/v$ and during an interval $\Delta t' = \Delta x/v$. Therefore we may write:

$$G(x,t) = \text{const}\,\Delta N^*(t - x/v) = \text{const}\,f(t - x/v)\,\dot{N}\Delta t',$$

$$g(x,t)\,\Delta x = \text{const}\,f(t - x/v)\,\dot{N}\Delta x/v.$$

Since $\dot{N}$ and v are assumed to be constants, it can be seen that:

$$g(x,t) = \text{const}\,f(t - x/v). \tag{2}$$

Therefore, the counts in the distal axon *reflect the state of the pool fraction at earlier times* and can thus be used to examine events within the cell soma. Since, from this viewpoint, the downflow serves merely to provide a transformation mechanism for intrasomal events, we can concentrate only on the function $f(t)$ and rely upon the transformation equation 2 to predict the activity profile in the axon.

As pointed out above, the exponential decay (Eq. (1)), is the simplest behavior for $f(t)$. It corresponds to an instantaneous loading of the pool at time $t = 0$ to a level f_o. More complex functions f can be built by using the principle of superposition. Consider a function $h(\tau)$ describing the input of activity to the pool: $\Delta N(\text{in}) = \dot{N}\Delta\tau$ and $\Delta N^*(\text{in}) = h(\tau)\,\Delta N = h(\tau)\dot{N}\Delta\tau$. The contribution to $f(t)$ of the portion of entering activity represented by $h(\tau)\,\Delta\tau$ is given by:

$$df(t) = \alpha h(\tau) d\tau e^{-\alpha(t-\tau)}; t \geq \tau.$$

By integrating over the variable τ, we therefore arrive at a complete expression for $f(t)$:

$$f(t) = \int_0^t \alpha h(\tau)\, e^{-\alpha(t-\tau)}\, d\tau. \tag{3}$$

A more revealing form can be obtained by factoring out a portion of the time dependence in Eq. 3 and rewriting it as:

$$f(t) = e^{-\alpha t} \int_0^t \alpha h(\tau) e^{\alpha\tau}\, d\tau = e^{-\alpha t} F(t)$$

where

$$F(t) = \int_0^t \alpha h(\tau) e^{\alpha\tau} \, d\tau . \tag{4}$$

In this form, the explicit dependence of $f(t)$ upon the exponential decay is displayed. In the case that the function $h(\tau)$ is essentially zero after a finite time T, the second factor $F(t)$ becomes a constant $F(T)$ for values of t beyond T, and then the time dependence of f is identical to Eq. 1.

The early time dependence of f is dominated by $h(\tau)$. This function represents the operation of a multiplicity of processes acting upon the injected radioactive precursor (usually amino acid) up to the formation of labeled protein and its entrance into the export pool. Despite this complexity it seems reasonable that, in general, $h(\tau)$ begins at a value of zero, rises to a peak, and then declines once again to zero, all within some finite time period denoted by the number T. Therefore, the function f is in this model described by only two parameters α and T; α describes that portion of Fig. 1 labeled C and T the portion labeled D.

The determination of a value for α is aided by the relatively large separation of the two times characteristic of the process. The slope at D is quite a bit steeper than the one at C which corresponds to the fact that $T < \alpha^{-1}$. Thus α can be estimated from the data by laying a straight edge along the portion labeled C (Fig. 1) and measuring the slope. Using this technique I have found values for α from several experimental

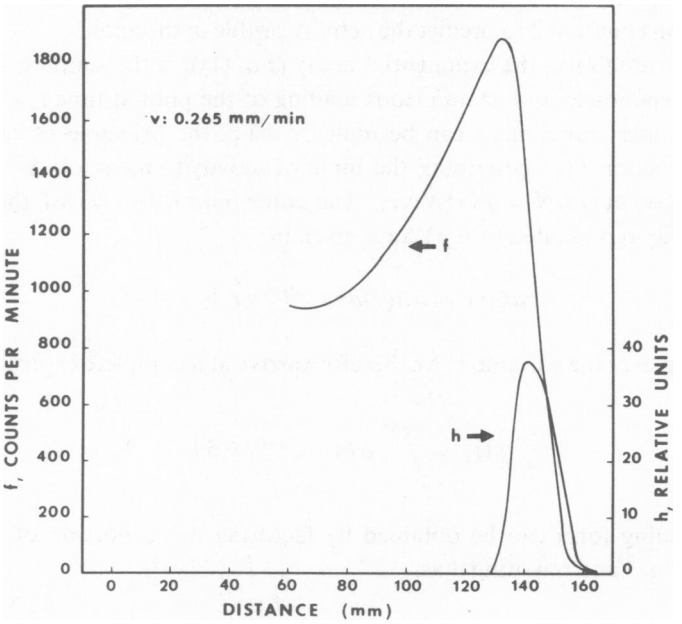

FIGURE 3 The functions f and h as defined in the text.

curves. These are approximately $\alpha = 0.004\ \text{min}^{-1}$ (or $\alpha^{-1} = 250$ min). An estimate for T is somewhat more difficult due to the interaction between the buildup of pool radioactivity and its export at the early times, and also because of the problem of deciding how to define the limiting points on the downflow profile. However, a crude estimate can be made from the "fall" time of this profile and this yields a value of $T \approx 90$ min. If a suitable form for the function $h(\tau)$ could be found from, for instance, theoretical considerations about the initial intrasomal processes leading to the formation of labeled molecules, this could be inserted into Eq. 4 and the result fitted to the observed data. Such an effort would yield estimates for whatever parameters were included in this formulation of $h(\tau)$. This mode of attack suffers from a lack of knowledge on how to develop an expression for h.

Alternatively, instead of trying to find an analytical form for $h(\tau)$ one can try the approach of unfolding the data and thereby arriving at a numerical form for h. This approach can be realized by differentiating Eq. 4 as follows. Let Δ represent an infinitesimal increment in t.

$$f(t+\Delta) = e^{-\alpha(t+\Delta)} \int_0^{t+\Delta} \alpha h(\tau) e^{\alpha\tau}\, d\tau = e^{-\alpha t} e^{-\Delta\alpha} \cdot \left\{ \int_0^{t} \alpha h(\tau) e^{\alpha\tau}\, d\tau + \int_t^{t+\Delta} \alpha h(\tau) e^{\alpha\tau}\, d\tau \right\}$$

$$= e^{-\alpha t} e^{-\Delta\alpha} \left\{ \int_0^{t} \alpha h(\tau) e^{\alpha\tau}\, d\tau + \alpha h(t') e^{\alpha t'} \Delta \right\}$$

$$= e^{-\alpha\Delta} \{ f(t) + h(t')\, \alpha\Delta \}; \qquad (t < t' < t + \Delta)$$

$$h(t') = \frac{f(t+\Delta) e^{\alpha\Delta} - f(t)}{\alpha\Delta}. \tag{5}$$

Using Eq. 5 the raw data can be processed to obtain a numerical representation for $h(t)$. A typical result of this is shown in Fig. 3. In this figure, the functions f and h have been transformed from their time-dependent forms into their space-dependent forms through the application of Eq. 2. $h(t)$ is seen to be a fairly sharply rising curve reaching its maximum amplitude about 35 min (10 mm/0.26 mm/min) before f, and then dropping down to zero somewhat more rapidly than it rose. The quantity T can be defined as the width of h at one-half its maximum value. This procedure leads to a value: $T = 60$ min. This form, and nearly the same values for the parameters, were found for several experiments differing only in the time elapsed between injection and sacrifice (smallest time: 5 h, longest time: 10 h). Data from similar experiments carried out using rats (I. Nadelhaft and F. Ronco, 1973, unpublished results) yielded comparable results but the data was not as suitable for analysis due to the relatively shorter available length of nerve.

The analysis presented here is a phenomenological analysis of the broad features of

the fast axoplasmic transport downflow profile. It conceives of the process as comprising two interconnected stages: (*a*) the manufacture of proteins and their storage in an export pool within the cell soma, and (*b*) the movement of these proteins out of the pool and distally along the axon.

The model does not attempt to account for the large amount of activity at the peak (A) of Fig. 1. This is probably associated with materials that either remain within the soma or are exported as the slowly flowing component. Since the slow component moves at a rate of approximately 1 mm/day, even fast flow data representing incubation times as long as 10 h should be completely free from interference by slowly flowing components. However, the slowly moving materials have been less thoroughly investigated than the rapidly flowing ones and it is possible that the slow flow is actually composed of a spectrum of several components each of which has a different speed. This possibility could account for the relatively broad base around the peak (A). Diffusion of precursor to non-neuronal cells local to the injection site can also contribute to a broad peak.

Speculation concerning a multiplicity of transport speeds can also be raised with regard to the fast-moving materials. Such a condition would have an effect on the advancing front of the downflow (D) in Fig. 1 and would tend to broaden it as the incubation time increased. Existing data suggest that this may be occurring to a small degree but more refined experiments involving greater precision and longer times are needed to clarify the question. In addition it is conceivable the speed of fast transport could vary from one axon to another depending on the cell type and/or the axonal diameter. These parameters are not sorted out in the gross experimental data that presently are available, but here again refinements including autoradiographic techniques and single cell injections may answer these questions.

I would like to thank Professors Allen Janis and Sidney Ochs for reading the manuscript and offering helpful comments on it.

Received for publication 26 April 1976.

REFERENCES

OCHS, S. 1972*a*. Rate of fast axoplasmic transport in mammalian nerve fibers. *J. Physiol. (Lond.).* **227**: 627.

OCHS, S. 1972*b*. Fast transport of materials in mammalian nerve fibers. *Science (Wash. D. C.).* **176**:252.

OCHS, S., M. I. SABRI, and N. RANISH. 1970. Somal site of synthesis of fast transported materials in mammalian nerve fibers. *J. Neurobiol.* **1**:329.